Liquid gallium-lead mixture spinodal, binodal, and excess thermodynamic properties

B. Grosdidier,[1] S. M. Osman,[2,*] and A. Ben Abdellah[1,3]

[1]*Laboratoire de Physique des Milieux Denses, Institut de Chimie, Physique et Matériaux, Université Paul Verlaine-Metz, 1 Boulevard Arago, 57078 Metz Cedex 3, France*

[2]*Physics Department, College of Science, Sultan Qaboos University, P.O. Box 36, Postal Code 123, Al-Khod, Muscat, Sultanate of Oman*

[3]*Electronics & Microwaves Group, UFR (Electronique et Physique du Solide), Faculty of Science, Abdelmalek Essaadi University, P.O. Box 2121, Tetuan 93000, Morocco*

(Received 27 April 2008; revised manuscript received 10 June 2008; published 16 July 2008)

A statistical mechanical based theory is developed for incorporating the effect of the long-range forces in Ga-Pb alloy. In particular, the simplified random-phase approximation is employed in conjunction with the Grosdidier *et al.* [Phys. Rev. B **72**, 024207 (2005)] model for GaGa and PbPb interactions while a suitable nonadditive pair potential is introduced between unlike atoms. We present analytical expressions for the equation of state and for the concentration fluctuations $S_{CC}(0)$, and then the role of the nonadditivity parameter is established by consulting the empirical critical parameters of the spinodal curve. It becomes possible to deduce the behavior of different thermodynamic functions such as Gibbs energy of mixing, excess Gibbs energy, isobaric heat capacity, and $S_{CC}(0)$ in the vicinity of the liquid-liquid critical point and under extremely high pressure. The impact of temperature and pressure on segregation, and compound-forming tendencies is also investigated. Moreover, the immiscibility gap of the alloy is calculated and compared with the empirical results. The results suggest that: (i) the nonadditivity of the potential tails plays a dominant role in the determination of the spinodal curve, (ii) $S_{CC}(0)$ is a very sensitive function in triggering the chemical short-range order, and (iii) the segregation or phase separation in Ga-Pb alloy is an outcome of the temperature dependence of the energy mismatch parameter. In conclusion, the present equation of state is sufficiently accurate that it provides a binodal curve, an excess Gibbs energy of mixing and isobaric heat capacity in quantitatively good agreement with the empirical results.

DOI: 10.1103/PhysRevB.78.024205 PACS number(s): 64.30.Ef, 64.75.Gh, 64.75.Op, 64.60.fh

I. INTRODUCTION

Liquid-liquid (*L-L*) phase equilibrium has become an important field of investigation in view of its extensive applications in analytical chemistry and in hydrocarbon industry. It is also essentially important in nuclear fuel processing and production.[1] In particular, Ga-Pb alloy enjoys special significance due to its cosmological and metallurgical relevance.[2] The phase diagram of Ga-Pb system was reported first by Puschin *et al.*[3] and Predel.[4] It shows monotectic and eutectic transitions at 590 and 302 K, respectively. Accurate isobaric heat-capacity measurements by Mathon *et al.*[5] have confirmed the monotectic parameters, $T=583.8$ K and gallium concentration $C_{\mathrm{Ga}}=0.0395$. The advanced differential thermal scanning calorimetry techniques enabled more precise measurements of the excess thermodynamics properties over the entire concentration range of the miscibility gap,[5,6] and accurate prediction of critical parameters $T_c=879.8$ K and $C_c^{\mathrm{Ga}}=0.532$. Quite recently, measurements of the electrical resistivity of Ga-Pb alloy under high pressure were carried out,[7,8] which showed a very large miscibility gap between 5.5 and 97.6 at % gallium with critical parameters $T_c=879.15$ K and $C_c^{\mathrm{Ga}}=0.6$. These measurements could also give evidence of the presence of rather flat *L-L* coexistence curve in the wide vicinity of the critical point. One of the reasons is that the metal-like bonds remains of the same type in both Ga-rich and Pb-rich coexisting liquids through the entire interval of the miscibility gap. On the other hand, the Ga-Pb alloy exhibits peculiar interfacial characteristics. A complete wetting transition at *L-L* coexistence for the alloy $Ga_{0.95}$-$Pb_{0.05}$ has been observed by Turchanin *et al.*[9] at temperatures in the range of 550–740 K. Also, prewetting of Pb-rich solid by Ga-rich liquid was reported by Cheng *et al.*[10] at temperatures between the eutectic and monotectic temperatures, where the liquid miscibility gap is metastable. The prewetting line is connected to the edge of the *L-L* coexistence line at the complete wetting transition temperature. In recent years, a growing interest in the surface freezing and surface melting transitions emerged at the liquid-vapor (*L-V*) interface in Ga-Pb mixture.[11] This was recently observed by means of x-ray measurement reflectivity[12] and second-harmonic generation (SHG) measurements.[13]

The theoretical basis of thermodynamic stability was first stated by Gibbs: a homogeneous phase with energy $G(C_1,T,P)$ is minimal at constant temperature T, pressure P, and independent concentration C_1. The concept of stability is normally related to specific case of phase equilibrium in which homogeneous and heterogeneous phases can coexist.[14] In order to establish the stability condition, we consider the Gibbs free energy of mixing, defined as

$$G_{\mathrm{mix}} = G - (C_1 G_1^0 + C_2 G_2^0) \leq 0, \tag{1}$$

where $C_2=1-C_1$ and G_i^0 refers to the Gibbs energy of pure components ($i=1$ and 2), all of which must be evaluated at the same T and P. The constraint in Eq. (1) indicates that mixing of fluids is only possible when G_{mix} is negative and homogeneous phase is obtained at every concentration; otherwise pure fluids will remain immiscible and no homoge-

neous mixture will be possible. In the case of partial miscibility, G_{mix} function has two inflection points and the concavity of G_{mix} changes with composition at constant T and P. Hence an additional miscibility test of binary alloys is obtained if $(\partial^2 G_{\mathrm{mix}}/\partial C_1^2)_{T,P,N}>0$. This follows from the fact that a system will always present instability if G_{mix} inflects. Applying this condition to Eq. (1) yields

$$\left(\frac{\partial^2 G}{\partial C_1^2}\right)_{T,P,N} > 0. \tag{2}$$

This condition indicates that $G(C_1,T,P)$ exhibits a positive concavity for the homogeneous mixture to be stable.[15] An alternative approach, originally put forward by Bhatia and Thornton,[16] and McAlister and Turner,[17] and successfully used by several authors,[18–22] is that the concentration fluctuations, $\langle \Delta C^2 \rangle$, is related to the concentration-concentration partial structure factor $S_{CC}(0)=\langle N\rangle\langle \Delta C^2\rangle$ at the long-wavelength limit, $q\to 0$. The Bhatia-Thornton structure factor $S_{CC}(q)$ has the advantage of easy identification either from the thermodynamics route,

$$S_{CC}(0) = N\left(\frac{\beta\partial^2 G}{\partial C_1^2}\right)_{T,P}^{-1}, \tag{3}$$

or from a statistical mechanical route (e.g., Bhatia[23]),

$$S_{CC}(q) = \frac{C_1 C_2}{1 - C_1 C_2 \rho[C_{11}(q) + C_{22}(q) - 2C_{12}(q)] - C_1 C_2 f(q)}, \tag{4}$$

where $\beta=(k_B T)^{-1}$, k_B is Boltzmann's constant, and $C_{ij}(q)$ are the familiar Orstein-Zernike direct correlation function. Equation (3) establishes the link between the stability function and $S_{CC}(0)$; therefore $S_{CC}(0)$ can be used to test the stability as well as the degree of immiscibility of binary mixture. Equation (3) has three important limits: (i) $S_{CC}(0)\to 0$ at the stoichiometric composition, (ii) $S_{CC}(0)\to\infty$, where the system approaches its critical point of demixing, T_C. Singh and Sommer[24] observed that the small increment of temperature of $\cong 10^{-2}$ K in the vicinity T_C may bring an increase in $S_{CC}(0)$ as large as $\cong 10^2$. (iii) The ideal mixture Gibbs free energy is normally defined as

$$\beta G_{id} = N(C_1 \ln C_1 + C_2 \ln C_2), \tag{5}$$

giving, via Eq. (3), the ideal mixing limit to the concentration fluctuations,

$$S_{CC}^{id}(0) = C_1 C_2, \tag{6}$$

which corresponds to random distribution of two types of atoms. The deviation from ideal mixing condition, $S_{CC}(0) < S_{CC}^{id}(0)$, indicates compound-forming tendency, i.e., unlike-atom pairs are preferred as nearest neighbors (heterocoordination). On the other hand, $S_{CC}(0)>S_{CC}^{id}(0)$ indicates phase-separating tendency or demixing state; in this case like-atoms tend to pair as nearest neighbors (homocoordination). Introducing the excess Gibbs energy $G_{ex}=G-G_{id}$ into Eq. (2) gives the definition of the so-called excess stability function, E_{ex}, that was originally introduced by Darken,[25] namely:

$$\beta E_{ex} = \frac{1}{S_{CC}(0)} - \frac{1}{C_1 C_2}. \tag{7}$$

Equation (4) is an exact relation. Three simplifying assumptions were imposed on Eq. (4) in order to interpret the chemical short-range order [CSRO] in binary alloys. First, the function $f(q)$ is assumed extremely small, which is typically the case for substitutional alloys such as Li-Ca alloy.[26–28] Second, the direct correlation function $C_{ij}(q)$ are simplified within Bhatia-Young model,[29] which is known as simplified random-phase approximation [SRPA]; in Fourier space it reads

$$C_{ij}^{\mathrm{SRPA}}(q) = C_{ij}^0(q) - \beta\tilde{\Phi}_{\mathrm{ord}}^t(q). \tag{8}$$

Here, $C_{ij}^0(q)$ represent the reference fluid direct correlation functions, which are normally the mixture of hard spheres, characterized with hard-sphere diameters σ_{ij} and $\Phi_{ij}^t(r)$, which are the long-range contributions to the pair interactions $\Phi_{ij}(r)$ at $r\geq\sigma_{ij}$. The third assumption was the definition of the ordering potential by Copestake *et al.*,[27]

$$\Phi_{\mathrm{ord}}(r) = \frac{1}{2}[\Phi_{11}(r) + \Phi_{22}(r)] - \Phi_{12}(r). \tag{9}$$

Then the approximation form of Eq. (4) for nearly symmetric mixture ($\sigma_{11}\approx\sigma_{22}$) yields the link between $\tilde{\Phi}_{\mathrm{ord}}(q)$ and $S_{CC}(q)$ at $q\to 0$ limit:

$$\rho\beta\tilde{\Phi}_{\mathrm{ord}}(0) = \frac{1}{2}\left[\frac{1}{S_{CC}(0)} - \frac{1}{C_1 C_2}\right], \tag{10}$$

with ρ being the number density. Equations (7) and (10) confirm that the two routes for calculating $S_{CC}(0)$ are equivalent. Also they emphasize the importance of $S_{CC}(0)$ in investigating the stability in binary mixtures with particular reference to segregation and CSRO.

Therefore, the condition of the critical point reads

$$S_{CC}(0)^{-1} = \left(\frac{\partial^2 \beta G}{\partial C_1^2}\right)_{C_1=C_{1c}} = \left(\frac{\partial^3 \beta G}{\partial C_1^3}\right)_{C_1=C_{1c}} = 0, \quad \text{at} \quad T=T_C. \tag{11}$$

In our investigation of Ga-Pb alloy, the quantity of central importance is $S_{CC}(0)$, which has strong concentration and temperature dependence for both cases of demixing and ordering. It is the T dependence of $S_{CC}(0)$ that allows us to calculate, with reasonable accuracy, the spinodal curve of Ga-Pb mixture at the entire concentration range and also locate precisely its critical parameters. The T dependence of $S_{CC}(0)$ comes originally from the strong T dependence of the potential parameters of pure constituents. Nowadays, there is increasing interest in exploring the possibility of fluid-fluid phase separation in systems with purely repulsive forces.[30] Square shoulder [SS] potential, which is a Silbert-Young model,[31] is a good candidate. Grosdidier *et al.*[32] employed SS model potential for calculating the structure factors $S_{ii}(q)$ of pure metals Ga and Pb within the level of accuracy of SRPA. The fitted $S_{ii}(q)$, with the empirical results, provide linear temperature dependence to the potential parameters at a temperature range covering the entire liquid phase of pure

Ga and Pb. In the present work, we employed Grosdidier *et al.*'s version of SS potential for like-atom interactions while for unlike-atom pairs, we used SS potential with additive core radius and nonadditive potential strength with nonadditivity parameter α. Actually, the latter assumption was introduced by our group in several papers.[18–22,33,34] The advantage of this approach lies in the simplicity of the expressions obtained for the properties of interest and that, at this level of description, the details of the potentials of different species in the alloy are not important since only the parameters of these potentials are important.

The layout of the paper is as follows. In Sec. II, we present the SS model potential and the analytical expression of the proposed equation of state (EOS) based on SRPA. In Sec. III we pursue the thermodynamic approach to obtain an analytical expression of $S_{CC}(0)$ and describe our method for the determination of the critical parameters, as well as the nonadditivity parameter α. Then we calculate the spinodal curve and compare it with the existing theoretical[32] and empirical results.[35] Also, the C, T, and P dependences of $S_{CC}(0)$ are discussed for both demixing and ordering tendencies with the help of our analytical expression. In Sec. IV we demonstrate the procedure for locating the liquid-liquid equilibrium [LLE] in binary mixtures and present the binodal curve of Ga-Pb alloy. Also the quality of the present EOS is checked by extensive comparison with the empirical results of the binodal curve, the excess Gibbs free energy of mixing, and the isobaric heat capacity. This is followed with concluding remarks in Sec. V.

II. PAIRWISE INTERACTIONS AND EQUATION OF STATE OF Ga-Pb MIXTURE

A. Model potential for Ga-Pb system

The constituent elements are assumed to be interacting via pair potentials $\Phi_{ij}(r)$, consisting of short-range repulsion, $\Phi_{ij}^{hs}(r)$, usually with the hard-sphere and weak long-range tail potentials, $\Phi_{ij}^{t}(r)$, namely:

$$\Phi_{ij}(r) = \Phi_{ij}^{hs}(r) + \Phi_{ij}^{t}(r). \tag{12}$$

With $i,j=1$ and 2 for Ga and Pb, respectively. The hard-sphere potentials are characterized with hard-core diameters σ_{ij},

$$\Phi_{ij}^{hs}(r) = \begin{bmatrix} \infty & r < \sigma_{ij} \\ 0 & r > \sigma_{ij} \end{bmatrix},$$

$$\Phi_{ij}^{t}(r) = \begin{bmatrix} 0 & r < \sigma_{ij} \\ \varepsilon_{ij} & \sigma_{ij} \le r \le \lambda_{ij}\sigma_{ij} \\ 0 & r > \lambda_{ij}\sigma_{ij} \end{bmatrix}. \tag{13}$$

The long-range contribution has been considered as the SS potential, which is often called Silbert-Young[31] potential. ε_{ij} and λ_{ij} represent the strength and range of the SS potential. ε_{ij} and λ_{ij} are assumed to be additive, that is, they obey the well-known Lorentz-Berthelot mixing rule, i.e.,

TABLE I. Fitting parameters of square shoulder potential for pure Ga and Pb.

Potential parameters	Gallium	Lead
σ^0(Å)	2.62709	3.15112
$\bar{\sigma}$(Å/K)	-1.37418×10^{-4}	-1.21235×10^{-4}
ε^0/k_B(K)	70.33	172.26
$\bar{\varepsilon}$	0.04667	–0.05456
λ^0	2.94929	1.89311
$\bar{\lambda}$(K^{-1})	2.94059×10^{-4}	1.76116×10^{-4}

$$\sigma_{12} = (\sigma_{11} + \sigma_{22})/2 \quad \text{and} \quad \lambda_{12} = (\sigma_{11}\lambda_{11} + \sigma_{22}\lambda_{22})/(2\sigma_{12}), \tag{14}$$

whereas the ε_{ij} is taken to be nonadditive, in violation to the mixing rule:

$$\varepsilon_{12} = \alpha(\varepsilon_{11}\varepsilon_{22})^{1/2}. \tag{15}$$

The parameter α is often called the nonadditivity parameter, which represents the relative strength of the unlike potential. Actually α was first introduced by Ichimura and Ueda[36] in their calculations of the phase diagram of square-well fluid mixture. This parameter controls the energetic of interactions among the constituent species. It has been reported recently[20–22] that the choice of α can account on the phase-separation or compound-forming tendencies for systems exhibiting strong chemical ordering. Quite recently, Grosdidier *et al.*[32] have used the SS potential for pure liquids Ga and Pb, and determined the potential parameters σ_{ij}, ε_{ij}, and λ_{ij} by consulting the observed structure factor of pure Ga, reported by Bellissent-Funel *et al.*,[37] and of pure Pb, reported by Dahlborg *et al.*[38] The fitting expressions are found to be linear functions of temperature, T, within the whole liquid range of Ga and Pb:

$$\sigma_{ii} = \sigma_{ii}^0 + \overline{\sigma_{ii}}T, \quad \varepsilon_{ii} = \varepsilon_{ii}^0 + \overline{\varepsilon_{ii}}k_BT \quad \text{and} \quad \lambda_{ii} = \lambda_{ii}^0 + \overline{\lambda_{ii}}T. \tag{16}$$

The fitting constants, as obtained by Grosdidier *et al.*,[32] are presented in Table I.

Here we are interested in the long-wavelength limit of the Fourier transform of the tail potential, $\tilde{\Phi}_{ij}^{t}(0)$, namely,

$$\tilde{\Phi}_{ij}^{t}(0) = 4\pi\int_0^\infty r^2\Phi_{ij}^{t}(r)dr. \tag{17}$$

For the SS potentials given by Eq. (13), the integrals are trivial:

$$\tilde{\varphi}_{ij}^{t}(0) = \frac{4\pi\varepsilon_{ij}\sigma_{ij}^3}{3}[\lambda_{ij}^3 - 1]. \tag{18}$$

Then, it is straightforward to obtain the relation of the $q \to 0$ limit for the ordering potential, $\tilde{\Phi}_{\mathrm{ord}}(0)$, as defined in Eq. (10) as

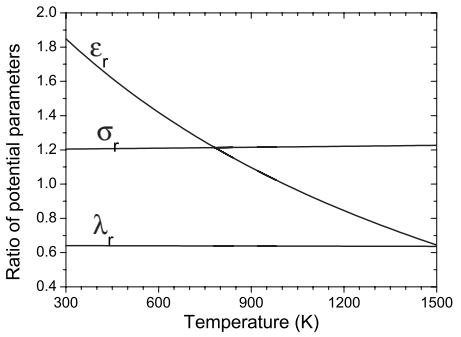

FIG. 1. Temperature dependence of size ratio $\sigma_r=\sigma_{22}/\sigma_{11}$, energy ratio $\varepsilon_r=\varepsilon_{22}/\varepsilon_{11}$, and range ratio $\lambda_r=\lambda_{22}/\lambda_{11}$ of the SS-potential parameters.

$$\tilde{\Phi}_{\mathrm{ord}}(0)=\frac{1}{2}[\tilde{\Phi}_{11}(0)+\tilde{\Phi}_{22}(0)]-\tilde{\Phi}_{12}(0). \tag{19}$$

Equations (19), (18), and (16) provide the T-dependent relation of the ordering potential via the potential parameters. Osman and Singh[19,20] investigated the role of the geometrical parameters σ_{ij}, ε_{ij}, and α on the phase stability of Lennard-Jones fluid mixtures. They observed that (i) the size mismatch, $\sigma_r=\sigma_{22}/\sigma_{11}$, alone is insufficient to bring segregation in binary mixture. (ii) The energy mismatch, $\varepsilon_r(=\varepsilon_{22}/\varepsilon_{11})$, as well as the nonadditivity parameter, α, clearly demonstrates a great impact on segregation or phase-separation tendencies. In order to investigate the role of σ_r and ε_r, as well as the range ratio $\lambda_r(=\lambda_{22}/\lambda_{11})$, we plotted the temperature dependence of these parameters for Ga-Pb alloy in Fig. 1 using the set of relations in Eq. (16). It shows clearly that both σ_r and λ_r have a very weak temperature dependence. Accordingly they may have no significant role on the phase separation of Ga-Pb mixture. On the other hand, the energy ratio, ε_r, shows dramatic decrease with increasing temperature, which reflects directly on the interchange energy ε_{12}. This strong temperature dependence of ε_{12} may interpret why segregation is achieved at low temperature while the mixture tends to have random mixing at $T\approx 1000$ K and may show the compound-forming tendency at lower temperatures.

All the potential parameters are impeded in the ordering potential, $\tilde{\Phi}_{\mathrm{ord}}(0)$, given in Eq. (19). Figure 2 shows clearly the temperature dependence of $\tilde{\Phi}_{\mathrm{ord}}(0)$. For $T<1040$ K, it shows $\tilde{\Phi}_{\mathrm{ord}}(0)<0.0$, which indicates that $\tilde{\Phi}_{12}(0)$ is more repulsive than the average of $\tilde{\Phi}_{11}(0)$ and $\tilde{\Phi}_{22}(0)$. This may interpret the origin of spinodal instability at lower temperatures. Conversely, positive $\tilde{\Phi}_{\mathrm{ord}}(0)$ at higher T corresponds to more gradual tendency toward ideal mixing.

B. Equation of state

According to Leonard-Barker-Henderson (LBH) thermodynamic perturbation theory,[39] all thermodynamic functions can be expressed in terms of reference system and perturbation contributions. The Helmholtz free energy per atom, F, and the pressure, P, are

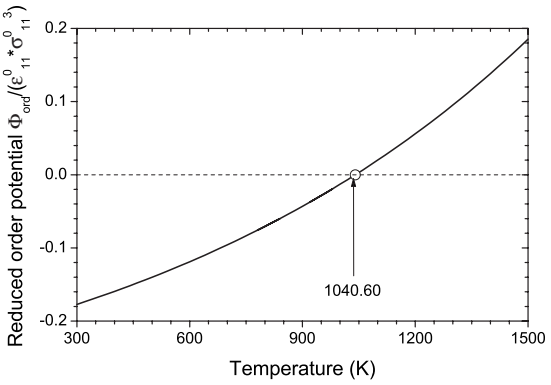

FIG. 2. The temperature dependence of the ordering potential, depicted from Eqs. (19), (18), and (16).

$$\beta F=\beta F_{hs}+\beta F_t \quad \text{and} \quad \beta P=\beta P_{hs}+\beta P_t. \tag{20}$$

Within the SRPA of Bhatia and Young,[29] the first-order perturbation contribution to the Helmholtz free energy is obtained from the long-wavelength limit of the Fourier transform of the tail potential, $\tilde{\Phi}^t_{ij}(0)$ namely:

$$\beta F_t=\frac{\rho\beta}{2}\sum_{i,j}C_iC_j\tilde{\Phi}^t_{ij}(0)$$

$$=\frac{\rho}{2k_BT}[C_1^2\tilde{\Phi}^t_{11}(0)+2C_1C_2\tilde{\Phi}^t_{12}(0)+C_2^2\tilde{\Phi}^t_{22}(0)]. \tag{21}$$

The tail contribution to the pressure, P_t, can be obtained immediately through the thermodynamic relation $\beta P_t=\rho^2(\partial\beta F_t/\partial\rho)_{T,C}$, which yields

$$\frac{\beta P_t}{\rho}=\beta F_t. \tag{22}$$

Returning now to the hard-sphere reference system formalism of P_{hs} and F_{hs}. We employ the recent modifications of the Boublik-Mansoori-Carnahan-Starling-Leland (BMCSL) expression for the pressure of the additive hard-sphere fluid mixture.[40,41] The modified expression is recently set by Barrio and Solana (BS) (Ref. 42) to account for the fourth and fifth virial coefficients, and satisfies the thermodynamic consistency condition. With these improvements, P_{hs} can be expressed as

$$\beta P_{hs}=\beta P_{hs}^{\mathrm{BMCSL}}+\beta P_{hs}^{BS}, \tag{23}$$

with

$$\frac{\beta P_{hs}^{\mathrm{BMCSL}}}{\rho}=\frac{1}{(1-\eta)}+\frac{3\eta_0y_1y_2}{(1-\eta)^2}+\frac{\eta_0^2y_2^3(3-\eta)}{(1-\eta)^3}, \tag{24}$$

and

$$\frac{\beta P_{hs}^{BS}}{\rho}=\frac{\eta_0^3Z}{(1-\eta)^2}, \tag{25}$$

where

$$Z = \xi_1 C_1 C_2 y_1 y_2 [y_4 + \xi_2]. \tag{26}$$

The subfunctions $\eta_0 = (\pi/6)\rho$, $y_n = C_1\sigma_{11}^n + C_2\sigma_{22}^n$, the packing fraction $\eta = \eta_0 y_3$, $\xi_1 = (\sigma_{11} - \sigma_{22})\sigma_{11}\sigma_{22}/\sigma_{12}$, and $\xi_2 = 2\sigma_{22}^2\sigma_{12}^2$. Having defined the pressure of hard-sphere mixture in Eq. (23), it is now possible to obtain the analytical expression for the excess Helmholtz free energy from the integral equation,

$$\beta F_{hs}^{ex} = \int_0^\rho \left(\frac{\beta P_{hs}}{\rho} - 1 \right) \frac{d\rho}{\rho}. \tag{27}$$

We carried out the integrations of Eqs. (24) and (25), the resulting expression is

$$\beta F_{hs}^{ex} = \left(\frac{2\eta_0^3 Z}{\eta^3} + \frac{\eta_0^2 y_2^3}{\eta^2} - 1 \right) \ln(1-\eta) + \frac{3\eta_0 y_1 y_2}{(1-\eta)} + \frac{\eta_0^3 Z(2-\eta)}{\eta^2(1-\eta)} + \frac{\eta_0^2 y_2^3}{\eta(1-\eta)^2}. \tag{28}$$

Then the Helmholtz free energy per atom of the hard-sphere references system can finally be written in terms of the ideal-gas contributions, F^{id}, and excess free energy, i.e.,

$$\beta F_{hs} = \beta F^{id} + \beta F_{hs}^{ex}, \tag{29}$$

with

$$\beta F^{id} = \sum_i C_i \ln C_i - \frac{3}{2}\sum_i C_i \ln m_i + \ln \rho - \frac{3}{2}\ln\left(\frac{k_B T}{\varepsilon_{11}}\right) + \frac{3}{2}\ln\left(\frac{h^2}{2\pi\varepsilon_{11}}\right) - 1. \tag{30}$$

where m_i denote the atomic masses of the constituent atoms and h is the Planck constant. Finally, other thermodynamic properties of interest follow from F and P. Thus the Gibbs free energy, G, is given as

$$\frac{\beta G}{N} = \frac{\beta F}{N} + \frac{\beta P}{\rho}. \tag{31}$$

III. CONCENTRATION FLUCTUATIONS AND THE SPINODAL CURVE

In this section we shall focus our attention on $S_{CC}(0)$ and present its analytical expression following the thermodynamic route given by Eq. (3). We perform the second derivative of Gibbs free energy [Eq. (31)] via Eqs. (20), (21), and (28)–(30), which is quite lengthy but worth presenting in a simplified form that we readily obtain

$$S_{CC}(0)^{-1} = S_{CC}^{id}(0)^{-1} + S_{CC}^{ex}(0)^{-1} + S_{CC}^{t}(0)^{-1}. \tag{32}$$

The ideal mixture contribution, $S_{CC}^{id}(0)$, is given in Eq. (6) while the tail contribution, $S_{CC}^{t}(0)$, can be obtained from Eq. (21) as

$$S_{CC}^{t}(0)^{-1} = \frac{\rho}{k_B T}[\tilde{\Phi}_{11}^{t}(0) + \tilde{\Phi}_{22}^{t}(0) - 2\tilde{\Phi}_{12}^{t}(0)] = \frac{2\rho}{k_B T}\tilde{\Phi}_{\mathrm{ord}}(0). \tag{33}$$

The second derivative of F_{hs}^{ex} [Eq. (28)] with respect to C_1 is done by tedious and simplified considerably to give $S_{CC}(0)^{-1}$ as

$$S_{cc}^{ex}(0)^{-1} = h_0 \ln(1-\eta) + \frac{h_1}{(1-\eta)} + \frac{h_2}{(1-\eta)^2} + \frac{h_3}{(1-\eta)^3} + \frac{h_4}{(1-\eta)^4}. \tag{34}$$

The values of which are

$$h_0 = \frac{6\eta_0^2 d_2^2 y_2}{\eta^2} + \frac{2\eta_0^3(Z_2 - 6d_1 d_2 y_2^2)}{\eta^3} + \frac{6\eta_0^4(d_3^2 y_2^3 - 2d_3 Z_1)}{\eta^4} + \frac{24\eta_0^5 d_3^2 Z}{\eta^5},$$

$$h_1 = 6\eta_0 d_1 d_2 + \frac{\eta_0^3[Z_2(2-\eta) - 6d_2 d_3 y_2^2]}{\eta^2},$$

$$h_2 = \eta_0^2 d_3(d_3 + 6\bar{y}) + \frac{6\eta_0^2 d_2^2 y_2}{\eta} - \frac{\eta_0^4 d_3[d_3 y_2^3(\eta^3 + 4\eta - 4) + 2Z_1(2\eta^2 - 9\eta + 6)]}{\eta^3},$$

$$h_3 = 6\eta_0^3 d_3^2 y_1 y_2 + \frac{6\eta_0^3 d_2 d_3(3\eta - 1)}{\eta^2} + \frac{2\eta_0^5 d_3^2 Z[4\eta^3 + 2\eta^2 - 11\eta + 6]}{\eta^4},$$

$$h_4 = \frac{2\eta_0^4 d_3^2 y_2^3(6\eta^2 - 4\eta + 1)}{\eta^3}.$$

Also,

$$Z_1 = \zeta_1[\bar{C} y_1 y_2 + C_1 C_2 \bar{y}(y_4 + \eta_2) + C_1 C_2 y_1 y_2 d_4],$$

and

$$Z_2 = 2\xi_1[(\bar{C}\bar{y} + C_1 C_2 d_1 d_2 - y_1 y_2)(y_4 + \xi_2) + (C_1 C_2 \bar{y} + \bar{C} y_1 y_2) d_4],$$

with $d_i = \sigma_{11}^i - \sigma_{22}^i$, $\bar{y} = y_1 d_2 - y_2 d_1$, and $\bar{C} = C_2 - C_1$.

Equation (32) together with Eqs. (6), (33), and (34) form the required analytical expression for $S_{CC}(0)$ related to the present EOS. One of the prime objectives in expressing $S_{CC}(0)$ in the present formula is that it can be used to investigate the role of temperature and pressure on the demixing properties of Ga-Pb mixture more accurately, and with less computational effort than carrying out the second numerical derivatives of Eq. (31).

In real system $S_{CC}(0)$ can lie anywhere between 0.0 to ∞, depending upon the physicochemical conditions of the mix-

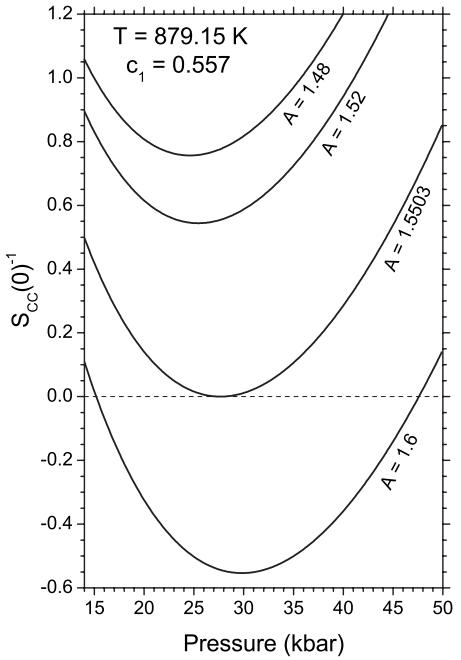

FIG. 3. Impact of the pressure and the nonadditivity parameter on the stability function, $S_{CC}(0)^{-1}$, at critical gallium concentration of $C_{1c}^{\mathrm{Ga}}=0.557$ and critical temperature of $T_c=879.15$ K (Ref. 35).

ture. The condition $S_{CC}(0)^{-1}\rightarrow 0$ determines the spinodal curve of the mixture. It is well known that the binodal and the spinodal curves for any fluid mixture coincide at the critical region. Therefore we use empirical binodal curve critical parameters available for Ga-Pb mixture,[35] $T_c=879.15$ K and $C_c^{Ga}=0.56$ then monitor the minimum of $S_{CC}(0)^{-1}$ versus pressure for several values of the nonadditivity parameters α. The critical pressure is achieved when $S_{CC}(0)^{-1}$ shows effectively its minimum with zero value in accordance with the critical condition specified in Eq. (11). It has been found that a unique pair (α, P_c) gives a precise zero for the minimum of $S_{CC}(0)^{-1}$. Figure 3 illustrates the influence of α on the minimum position. We found that the value of the empirical critical concentration, C_{1c}, must slightly be altered by 0.003 to satisfy exactly the necessary critical conditions, $[S_{CC}(0)^{-1}]_{\min}=0$, which uniquely determines the critical pressure $P_c=27.6644$ kbars, critical concentration $C_c^{Ga}=0.557$, and $\alpha=1.5503$. Grosdidier *et al.*[32] performed similar calculations for the same pair potential, as in Eq. (13), with exactly the same temperature dependent parameters σ_{ij}, ε_{ii}, and λ_{ij}, provided in Table I. These authors obtained $\alpha=1.4886$ and $C_{1c}=0.6231$ for the same value of $T_c=879.15$ K. The discrepancies between the two results of α and C_{1c} came originally from the different routes of describing the critical demixing condition. Grosdidier *et al.*[32] employed the stability matrix approach, which is based on the partial structure factors $S_{ij}(q)$ calculated within SRPA. In this approach, the mixture density as a function of temperature, $\rho(T)$, is an input quantity, which was basically composed from the empirical densities of the pure metals, $\rho_{Ga}(T)$ and $\rho_{Pb}(T)$, which were taken from Crawley[43] fitting formula. Their approach does not guarantee the fixed pressure condition, which is an essential condition for calculating $S_{CC}(0)$

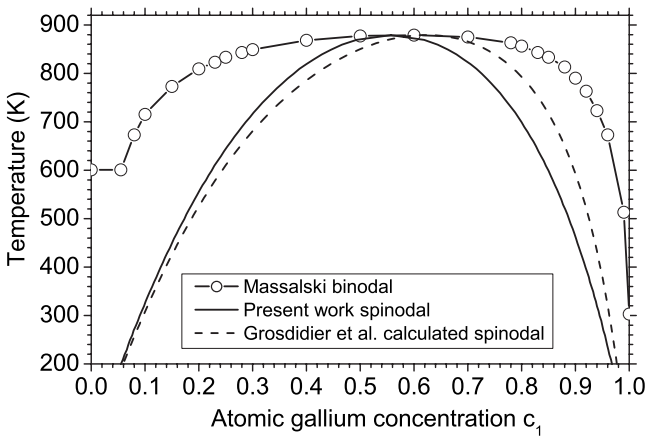

FIG. 4. Comparison of the calculated spinodal curves, the present work (full line) with theoretical calculations (Ref. 32) (dashed line), and the empirical binodal curve (Ref. 35) (circles).

and consequently for the spinodal curve calculations. In the present approach we used the thermodynamic route to the EOS that facilitates the determination of $\rho(C_1,T)$ self consistently at fixed pressure, P, from Eqs. (20), (22), and (23).

By determining the nonadditivity parameter α, and the critical parameters C_{1c} and P_c, it becomes possible now to calculate the spinodal curve with high precision by fixing, P, and searching for gallium concentrations C_1' and C_1'', which anole $S_{CC}(0)^{-1}$ for each temperature. Each pair (C_1', C_1'') with $C_1'<C_{1c}<C_1''$ specifies the miscibility gap at a given temperature. The whole picture of the spinodal curve in the temperature range $300\ \mathrm{K}<T<T_c$ is presented in Fig. 4 together with Grosdidier *et al.*'s[32] spinodal and the empirical binodal curves (Ref. 35). Grosdidier *et al.*'s spinodal shows an overestimation of the critical concentration by 11.3% while our critical composition is 0.5% lower than the experimental value. For all $T<T_c$ the binodal curve is wider than the spinodal. This is due to the thermodynamic condition imposed in each curve as the former gives the boundary of phase equilibrium while the latter shows the boundary of phase stability.

According to Eqs. (7) and (10), we suggest using the excess concentration fluctuations $S_{CC}^*(0)=S_{CC}(0)/S_{CC}^{id}(0)$, which measures the deviation from ideal mixing condition. Demixing is signaled by a strong enhancement of $S_{CC}^*(0)$ from 1.0. This is of great significance for visualizing the degree of CSRO in the mixture. If, at a given composition, $S_{CC}^*(0)>1.0$, then there is a tendency for segregation or phase separation.[44] On the other hand, $S_{CC}^*(0)<1.0$ is an indication of strong association, or the existence of chemical complex or what is known as a compound formation. In what follows we discuss the behavior of $S_{CC}^*(0)$ in the vicinity of the critical point. In Fig. 5, we present $S_{CC}^*(0)$ versus gallium concentration at the critical pressure $P_c=27.6644$ kbars for several isotherms. For $T<T_c$, $S_{CC}^*(0)$ exhibits phase separation and for $T>T_c$ the system inhibits concentration fluctuations going toward ideal mixing. The asymmetry in $S_{CC}^*(0)$ is independent of the temperature and is always at $C_1\approx 0.56$ in Ga-rich side, which is exactly the same as C_{1c}.

One of the basic advantages of the present approach is that it allows us to study the effect of temperature and pres-

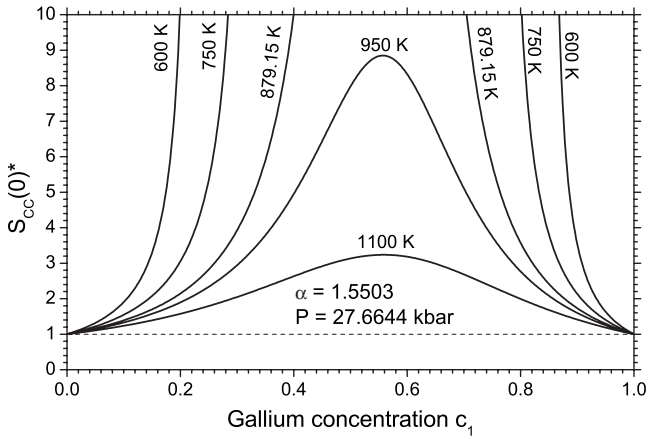

FIG. 5. Effect of temperature on the concentration fluctuation in the long-wavelength limit $[S^*_{CC}(0)=S_{CC}(0)/S^{id}_{CC}(0)]$ for Ga-Pb mixture as a function of gallium concentration at fixed pressure P_c =27.6644 kbars.

sure on segregation and compound-formation tendencies of Ga-Pb alloy through $S^*_{CC}(0)$, which is more sensitive to T and P than the excess thermodynamic functions. We plotted $S^*_{CC}(0)$ for $Ga_{0.56}$-$Pb_{0.44}$ mixture in Figs. 6 and 7, respectively. It is obvious from Fig. 6 that the more the pressure lowers, the more the segregation tendency enhances. The maximum $S^*_{CC}(0)$ is almost at P_c for all isotherms. The crossover to compound-forming region $[S^*_{CC}(0)<1.0]$ occurs roughly at 80 kbars. It seems that the short-range order prevails to the same effect in both the segregation and compound-forming regions in the vicinity of the crossover pressure. Figure 7 provides further illustration of the impact of temperature on $S^*_{CC}(0)$ at low-pressure range $(P\leq P_c)$ [Fig. 7(a)] and at higher pressures $(P>P_c)$ [Fig. 7(b)]. $S^*_{CC}(0)$ shows segregation tendency at all temperatures in Fig. 7(a) while the gradient $(\partial S^*_{CC}(0)/\partial T)_P$ is always negative and decreases with decreasing pressure. Eventually, the mixture reaches its ideal mixing state at extremely high temperatures. This is the characteristic feature of most phase-separating liquid mixtures for which the energy mismatch ε_r and the nonadditivity parameter α are playing a dominant role.[19] The most interesting behavior of $S^*_{CC}(0)$ can be seen

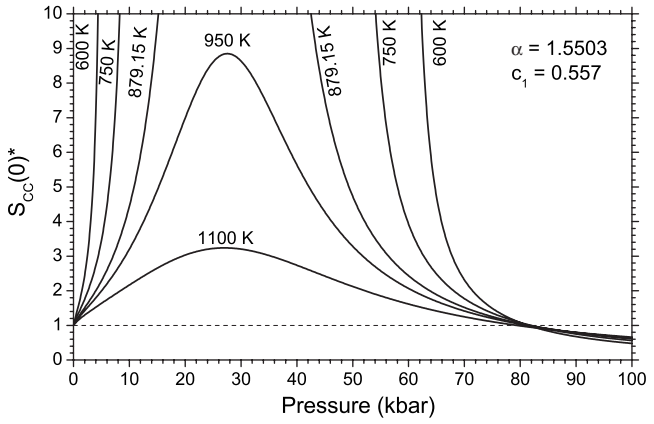

FIG. 6. The impact of pressure on $S^*_{CC}(0)$ for $Ga_{0.557}$-$Pb_{0.443}$ alloy at several isotherms.

in Fig. 7(b): At intermediate pressures $(P_c<P<75$ kbars), $S^*_{CC}(0)$ shows a crossover from segregation to compound-formation regions. The crossover temperature decreases by increasing pressure. Also it is interesting to observe the decrease in short-range order by increasing pressure. This behavior can be attributed to the reduction in the enthalpic effect on demixing due to the sharp decrease in energy ratio ε_r with increasing T, as observed in Fig. 1, which in turn reflects on switching of the ordering potential $\tilde{\Phi}_{\rm ord}(0)$ from negative to positive, as shown in Fig. 2. It is obvious from the approximate relation [Eq. (10)] and our complete formula [Eqs. (32) and (33)] that $\tilde{\Phi}_{\rm ord}(0)$ and $S^*_{CC}(0)$ are linked, and the sign change of $\tilde{\Phi}_{\rm ord}(0)$ is responsible on the crossover of $S^*_{CC}(0)$. The fact that Eq. (19), for $\tilde{\Phi}_{\rm ord}(0)$, has no concentration dependence and shows single zero at 1040 K forces $S_{CC}(0)$ to have a sign crossover that could be independent of the pressure value, which is not the case in Fig. 7(b). This is a strong indication that the approximation, $f(q)=0$, in Eq. (4) may not be totally valid for Ga-Pb alloy, otherwise $\tilde{\Phi}_{\rm ord}(0)$ should have a concentration dependence. We recall that such a crossover of $S^*_{CC}(0)$ was observed in several real systems, for example, Bi-Zn, Li-Sn, and Li-Pb.[24] (ii) At considerably higher pressures $(P>75$ kbars), $S^*_{CC}(0)$ indicates compound-forming tendency for the whole temperature range and gradient $(\partial S^*_{CC}(0)/\partial T)_P$ changes sign. Also, the asymmetry of $S^*_{CC}(0)$ changes its position. This behavior can be interpreted as an outcome of the enhancement of the entropic effects of the hard-sphere reference system more than the energetic effects due to the tail interactions. The characteristic features of $S^*_{CC}(0)$, presented in Figs. 5–7, can be utilized to understand the nature of bonding in Ga-Pb mixture within the vicinity of its critical end point. $S^*_{CC}(0)>1.0$ indicates self coordination and like atoms are in pairs as nearest neighbors, which signifies homocoordination. This segregation effect is enhanced dramatically by lowering either the temperature or the pressure below the critical value. On the other hand $S^*_{CC}(0)<1.0$ indicates heterocoordination, namely unlike atoms prefer to be in pairs at nearest neigh-

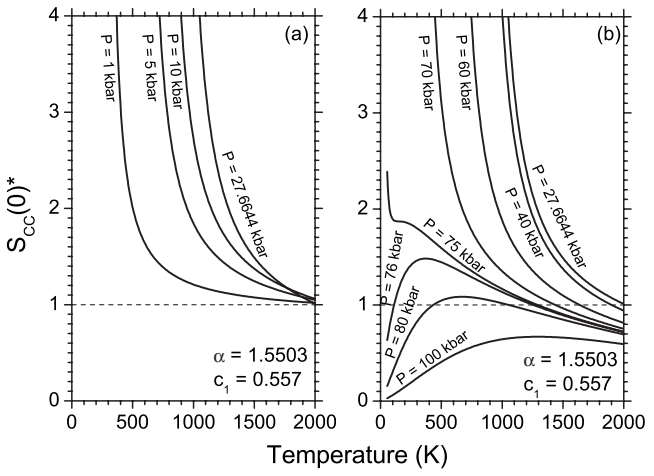

FIG. 7. Concentration fluctuations $S^*_{CC}(0)$ versus temperature for $Ga_{0.557}$-$Pb_{0.443}$ alloy at (a) low pressures, $P\leq P_c$ (=27.6644 kbars), and (b) high pressures, $P\geq P_c$.

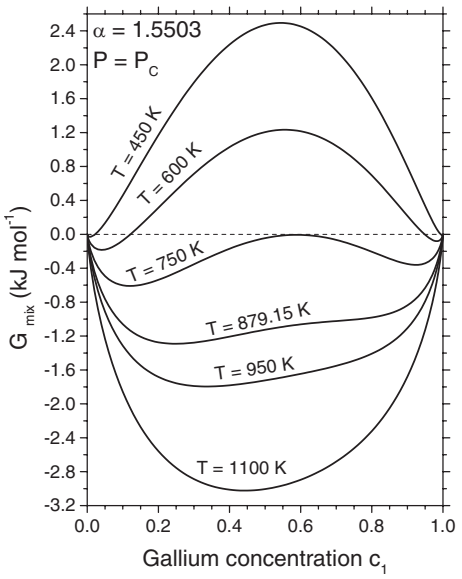

FIG. 8. Gibbs free energy of mixing, G_{mix}, as a function of Ga concentration for different isotherms.

bors. This effect is enhanced only by increasing pressure.

IV. THERMODYNAMIC PROPERTIES OF Ga-Pb ALLOY

Having defined the various contributions to the Gibbs free energy, G, in Sec. II, one can readily obtain an expression for the free energy of mixing, G_{mix}, as defined in Eq. (1). For calculating G_{mix} via Eqs. (1) and (31), one has to be careful as $G_i^0 = G(C_j \rightarrow 0)$ are the Gibbs free energies per atom for the two pure species Ga and Pb at the same pressure and temperature, as for the mixture. The general trend of the effect of temperature on G_{mix} is displayed in Fig. 8. The isotherm $T=1100$ K illustrates a case of complete miscibility for every composition. A negative value of G_{mix} is achieved, indicating that the mixture is in homogeneous phase. On the other hand, the curve for $T=450$ K represents a case of complete immiscibility, which, at every composition, yields a positive value of G_{mix}, indicating that the mixing process is impossible because it violates the stability constraint, $G_{\mathrm{mix}} < 0$. In this particular case the two phases are present with each corresponding to a pure component. The isotherms 600 K $\leq T <$ 950 K represent a case of partial miscibility while the G_{mix} function reveals two minima and concavity construction, which changes with temperature. The common tangent criteria can be applied for the two minima to give the compositions of the two liquid phases at equilibrium a particular T and P pair. The common tangent rule is often called the thermodynamic condition for phase coexistence, which provides the whole picture of the phase diagram. For more detail, we refer the reader to Ref. 14. The particular isotherm $T=879.15$ K shows a very shallow dip in G_{mix}, indicating that the two minima are conserving to one global minimum, which corresponds to the critical isotherm for which the critical composition can also be determined, as illustrated in Sec. III.

The double-minimum construction appearing in Fig. 8 suggests the possibility of calculating the liquid-liquid coexistence curve, which is normally called the LLE or the binodal curve. The main idea is to search for a common tangent for the two minima of each isothermal-isobaric G_{mix} versus C_1 curve. Such numerical procedure allows projecting the equilibrium compositions C_1^I and C_1^{II} of the two coexisting liquid phases I and II, respectively, in a $T-C_1$ diagram. Although, this procedure is not very accurate, it allows an easy visualization of the equilibrium behavior and its relation with the global stability of the alloy. In addition, it may be used for initializing rigorous calculations that usually are nonlinear. The alternative procedure may give place to the condition of equal chemical potential of each component of the alloy in phase I and in phase II, which are in equilibrium at the same pressure and temperature. This condition may be expressed as

$$\mu_i^I(C_1^I, T, P) = \mu_i^{II}(C_1^{II}, T, P). \tag{35}$$

The analytical expressions of the chemical potentials μ_1 and μ_2 can be found from the Gibbs free energy [Eq. (31)] according to the standard thermodynamic relations,

$$\mu_1(C_1, T, \rho) = G + C_2\left(\frac{\partial G}{\partial C_1}\right)_{T,P}, \tag{36}$$

and

$$\mu_2(C_1, T, \rho) = G - C_1\left(\frac{\partial G}{\partial C_1}\right)_{T,P}. \tag{37}$$

The derivative $(\partial G/\partial C_1)_{T,P}$ is also available in analytical form as it appears as part of the analytical expression of $S_{CC}(0)^{-1}$. With the help of the pressure equation [Eq. (20)], $\mu_i(C_1, T, \rho)$ can be transformed to $\mu_i(C_1, T, P)$. Finally, for each pair of P and T, the two nonlinear equations of $\mu_1(C_1, T, P)$ and $\mu_2(C_1, T, P)$ have to be solved iteratively to give three values of concentration $\{C_1', C_1'', C_1'''\}$ for fixed μ_1, and another three values $\{C_1^{\cdot}, C_1^{\cdot\cdot}, C_1^{\cdot\cdot\cdot}\}$ for fixed μ_2. Normally, the middle values $\{C_1'', C_1^{\cdot\cdot}\}$ are discarded as they refer to the unstable thermodynamic state. There exist the uniquely determined pair $\{C_1' = C_1^{\cdot}\}$ and $\{C_1''' = C_1^{\cdot\cdot\cdot}\}$ that satisfy the equilibrium condition [Eq. (35)], which also locate the equilibrium concentrations of the coexisting liquid phases, C_1^I and C_1^{II}, respectively. Repeating the procedure for various temperatures, we obtain the whole picture of the binodal curve at $P=P_c$, which, typically, corresponds to the set of curves in Fig. 8. We present our calculated binodal curve compared to the empirical results in Fig. 9. The agreement is excellent except in the vicinity of the critical point, which is due to the failure of the chemical-potential functions of showing inflection point at this temperature range. In general, this is an inherited problem for all equations of state that are based on the mean-field approximation. This also explains the reason why we used the spinodal curve to fit the critical point instead of using the binodal curve. For more details on the phase diagram calculations, we refer the reader to Refs. 18 and 36.

Now we turn back to fundamental function, the free energy of mixing, G_{mix}, given in Eq. (1), which is correlated

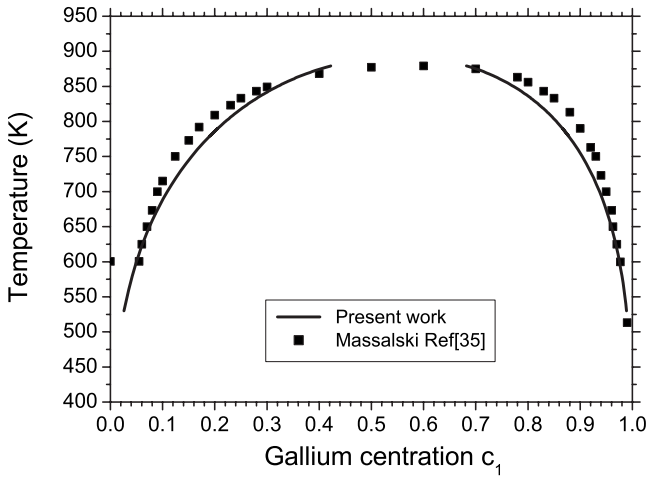

FIG. 9. Comparison of the calculated binodal curves using the present EOS (full line) with the empirical binodal curve (Ref. 35) (solid squares).

with the excess free energy of mixing G_{XS} via the standard definition

$$G_{XS} = G_{\text{mix}} - k_B T(C_1 \ln C_1 + C_2 \ln C_2). \tag{38}$$

The condition for ideal mixture can also be deducted from Eqs. (1), (5), and (38), $G_{XS}^{id}=0$. Hence, for ordering phase [preference of unlike atoms (GaPb) bonding as neighbors], $G_{XS}<0$. On the other hand, $G_{XS}>0$ indicates segregation [preference for like atoms (GaGa or PbPb) bonding as neighbors]. To check whether we may have some degree of confidence on the accuracy of the present EOS, we consider G_{XS} and the isobaric specific-heat capacity, C_p. The comparison of G_{XS} with the experimental results of Ansara and Ajersch[6] is presented in Fig. 10. A very good agreement is observed in the vicinity of T_c for $T=900$ K and 800 K while the agreement is less for more deviation from T_c.

The isobaric heat capacity, C_p, can be calculated via a numerical derivative of Eq. (31),

$$C_P = -T\left(\frac{\partial^2 G}{\partial T^2}\right)_{C,P} = -T\left[\frac{\partial^2}{\partial T^2}(F^{id} + F_{hs}^{ex} + F_t)\right]_{C,P} + TP\left[\frac{1}{\rho^2}\left(\frac{\partial^2 \rho}{\partial T^2}\right)_{C,P} - \frac{2}{\rho^3}\left(\frac{\partial \rho}{\partial T}\right)_{C,P}^2\right]. \tag{39}$$

We may recall that the variation of F and P are functions of σ_{ij}, ε_{ij}, and λ_{ij}, which in our scheme are T dependent, and hence contribute to entropy and heat capacity. The numerical derivative of various F contributions in Eqs. (21) and (28)–(30) can be obtained. $(\partial\rho/\partial T)_{C,P}$ and $(\partial^2\rho/\partial T^2)_{C,P}$ can be obtained via Eq. (17) at fixed P and C_1. The comparison of our prediction of C_P with experimental results is shown in Fig. 11. An excellent agreement between calculated values of isobaric heat capacity and experimental data is observed for a wider temperature range.

V. CONCLUSIONS AND PERSPECTIVES

An improved version of the EOS of liquid mixtures has been developed to study the thermodynamic stability of

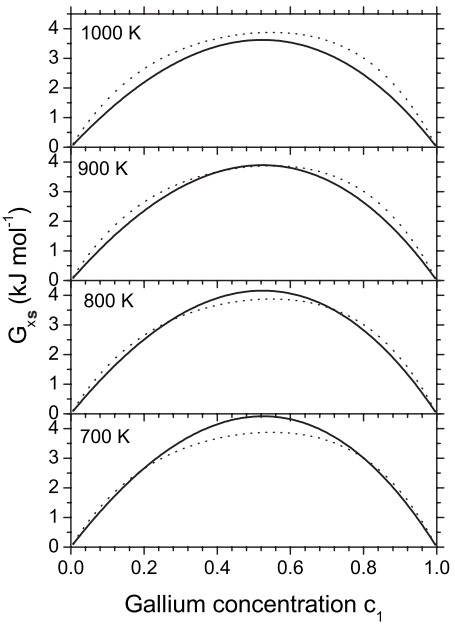

FIG. 10. Comparison between the calculated excess Gibbs free energy of mixing [Eq. (38)] (solid line) and the experimental data (dashed line) (Ref. 6) at four isotherms.

Ga-Pb liquid mixture. The EOS is formatted on the basis of statistical mechanical perturbation theory, in particular, the SRPA in which the correlation, $g_{ij}(r)$, due to long-range forces among the mixture species, have set equal unity while the main contributions from the long-range forces are taken through the SS potentials, which act as perturbation to the reference system. An analytical expression for the EOS of Ga-Pb system was presented. This, in turn, is used to obtain the analytical expressions for all thermodynamic functions of interest, as well as $S_{CC}(0)$. Moreover, the EOS has been

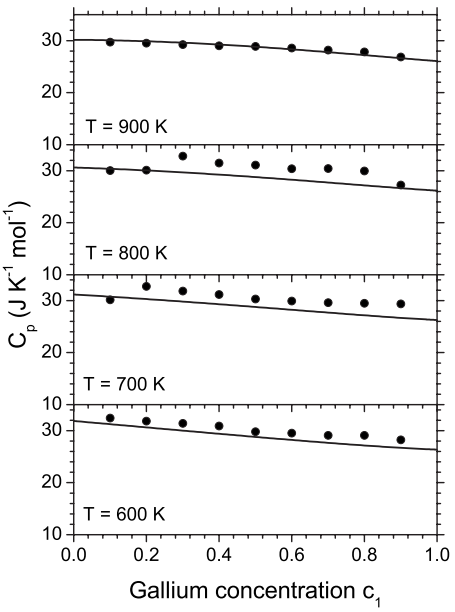

FIG. 11. Calculated molar heat capacity at constant pressure [Eq. (39)] (solid line) compared to the empirical values (Ref. 5) (solid circles) at different isotherms.

solved numerically at a given T and P to give the mixture density as a function of concentration, which guarantee the internal consistency of various variables. This enabled us to examine the role of temperature on various thermodynamic functions at low and high pressures regions, and also the impact of pressure at different isotherms.

The main results of the present work are as follows. From theoretical point of view, the most important conclusion is that an analytical expression of $S_{CC}(0)$ is obtained. Our formalism enables us to study the impact of different quantities, such as energy mismatch and ordering potential, on demixing and on short-range ordering in Ga-Pb mixture. The point of interest revealed in the present work is that the nonadditive energy parameter, α, was found to be a crucial trigger for the critical point and it plays an important role in precise determination of the spinodal curve of the alloy. In general, however, quite falling in the line, the observations of Grosdidier *et al.*[32] regarding the spinodal instability is interesting. These authors concluded that the origin of instability is mainly due to the depletion of the interaction between unlike atoms. We have performed an accurate estimation of the critical parameters for Ga-Pb mixture $T_c=879.15$ K, $P_c=27.6644$ kbars, and $C_c^{Ga}=0.557$, which correspond to a unique value of $\alpha=1.5503$. These calculations are based on the numerical search for global zero minimum of the stability function $S_{CC}(0)^{-1}$. Our results of $S^*_{CC}(0)$ clearly illustrate how the interplay of temperature and pressure affects the segregation and the compound-formation tendencies in Ga-Pb mixture. Although the results of $\tilde{\Phi}_{\mathrm{ord}}(0)$, G_{mix}, G_{XS}, and $S^*_{CC}(0)$ are consistent, $S^*_{CC}(0)$ is the most sensitive and useful function used to study the demixing or short-range order in the mixture. The obvious conclusion is that the purely repulsive potentials such as the SS model potential mixed with nonadditivity parameter, $\alpha>1.0$, is capable of reproducing liquid-liquid phase equilibrium. We also found that the present EOS is accurate enough to predict binodal curve, G_{XS}, and C_p in excellent agreement with empirical results over an extended region of temperature (600–1000 K). The agreement gives us confidence in our approach, and suggests that the present EOS can be used to calculate other transport and surface properties of Ga-Pb alloy. Work along this line is currently in progress.[45]

ACKNOWLEDGMENTS

We would like to thank J. G. Gasser for useful discussions and valuable suggestions. Two of us (S.M.O. and A.B.A.) thank the University Paul Verlaine-Metz for providing financial support and hospitality during our research visit when most of this work was carried out. This work was partially supported by the Sultan Qaboos University Grant No. IG/SCI /PHYS/03/04.

*Corresponding author. osm@squ.edu.om

[1] Y. Marcus and A. S. Kartes, *Ion Exchange and Solvent Extraction of Metals Complexes* (Wiley, New York, 1969).
[2] A. A. Nepomnyash Chy, M. G. Velarde, and P. Colinet, *Interfacial Phenomena and Convection* (Chapman and Hall, London, 2002).
[3] N. A. Puschin, S. Stepanovic, and V. Stajic, Z. Anorg. Chem. **209**, 329 (1932).
[4] B. Predel, Z. Metallkd. **50**, 632 (1959).
[5] M. Mathon, J. M. Miame, P. Gaune, M. Gambino, and J. P. Bros, J. Alloys Compd. **237**, 155 (1996).
[6] I. Ansara and F. Ajersch, J. Phase Equilib. **12**, 73 (1991).
[7] B. Sokolovskii, Yu. Plevachuk, and V. Didoukh, Phys. Status Solidi A **148**, 123 (1995).
[8] A. Ben Abdellah, J. G. Gasser, A. Makradi, B. Grosdidier, and J. Hugel, Phys. Rev. B **68**, 184201 (2003).
[9] A. Turchanin, R. Tsekov, and W. Freyland, J. Chem. Phys. **120**, 11171 (2004).
[10] Wei-Chun Cheng, Dominique Chatain, and Paul Wynblatt, Surf. Sci. **327**, L501 (1995).
[11] W. Freyland, A. H. Ayyad, and I. Mechdiev, J. Phys.: Condens. Matter **15**, S151 (2003).
[12] B. Yang, D. Gidalevitz, Huang Li, and S. A. Rice, Proc. Natl. Acad. Sci. U.S.A. **96**, 13009 (1999).
[13] A. Turchanin, W. Freyland, and D. Nattland, Phys. Chem. Chem. Phys. **4**, 647 (2002).
[14] H. Segura, Ilya Polishuk, and Jaime Wisniak, Z. Metallkd.Phys. Chem. Liq. **38**, 277 (2000).
[15] S. Rowlinson, *Liquid and Liquid Mixtures*, 3rd ed. (Butterworth, London, 1982).
[16] A. B. Bhatia and D. E. Thornton, Phys. Rev. B **2**, 3004 (1970); **4**, 2325 (1971).
[17] S. P. Mc Alister and R. Turner, J. Phys. F: Met. Phys. **2**, L51 (1972).
[18] S. M. Osman and M. Silbert, Phys. Chem. Liq. **23**, 239 (1991).
[19] S. M. Osman and R. N. Singh, Phys. Rev. E **51**, 332 (1995).
[20] S. M. Osman and R. N. Singh, Mol. Phys. **96**, 87 (1999).
[21] I. Ali, S. M. Osman, N. Solaiman, and R. N. Singh, Mol. Phys. **101**, 3239 (2003).
[22] I. Ali, S. M. Osman, N. Sulaiman, and R. N. Singh, Phys. Rev. E **69**, 056104 (2004).
[23] A. B. Bhatia, Inst. Phys. Conf. Seri. No. 30 (Institute of Physics, London, 1977), Chap. 1, Pt. 1, p. 21.
[24] R. N. Singh and F. Sommer, Z. Metallkd. **83**, 7 (1992).
[25] L. S. Darken, Trans. Metall. Soc. AIME **80**, 239 (1967).
[26] P. Chieux and H. Ruppersberg, J. Phys. (Paris), Colloq. **41**, C8-145 (1980).
[27] A. P. Copestake, R. Evans, H. Ruppersberg, and W. Schirmacher, J. Phys. F: Met. Phys. **13**, 1993 (1983).
[28] R. J. Bowles and M. Silbert, J. Phys. F: Met. Phys. **15**, L105 (1985).
[29] A. B. Bhatia and W. H. Young, Phys. Chem. Liq. **14**, 47 (1984).
[30] M. Rovere and G. Pastore, J. Phys.: Condens. Matter **6**, A163 (1994).
[31] M. Silbert and W. H. Young, Phys. Lett. **58A**, 469 (1976).
[32] B. Grosdidier, A. Ben Abdellah, and J. G. Gasser, Phys. Rev. B **72**, 024207 (2005).
[33] I. Ali, S. M. Osman, and R. N. Singh, J. Non-Cryst. Solids **250-**

252, 360 (1999).
[34] N. Sulaiman, S. M. Osman, I. Ali, and R. N. Singh, J. Non-Cryst. Solids **312-314**, 227 (2002).
[35] T. B. Massalski, H. Okamoto, P. R. Subramanian, and L. Kacprzak, *Binary Alloys Phase Diagrams* (ASM, Metals Park, OH, 1990).
[36] T. Ichimura and A. Ueda, J. Chem. Phys. **74**, 3566 (1981).
[37] M. C. Bellissent-Funel, P. Chieux, D. Levesque, and J. J. Weis, Phys. Rev. A **39**, 6310 (1989).
[38] U. Dahlborg, M. Davidovic, and K. E. Larsson, Phys. Chem. Liq. **6**, 149 (1977).
[39] P. J. Leonard, D. Henderson, and J. A. Barker, Trans. Faraday Soc. **66**, 2439 (1970).
[40] T. Boublik, J. Chem. Phys. **53**, 471 (1970).
[41] G. A. Mansoori, N. F. Carnahan, K. E. Starling, and T. W. Leland, J. Chem. Phys. **54**, 1523 (1971).
[42] C. Barrio and J. R. Solana, J. Chem. Phys. **113**, 10180 (2000).
[43] A. F. Crawley, Int. Metall. Rev. **19**, 32 (1974).
[44] R. N. Singh and F. Sommer, Rep. Prog. Phys. **60**, 57 (1997).
[45] S. M. Osman, B. Grosdidier, and A. Ben Abdellah (unpublished).